Mitochondrial targeting of recombinant RNAs modulates the level of a heteroplasmic mutation in human mitochondrial DNA associated with Kearns Sayre Syndrome

Caroline Comte[1&], Yann Tonin[1&], Anne-Marie Heckel-Mager[1], Abdeldjalil Boucheham[1], Alexandre Smirnov[1§], Karine Auré[2#], Anne Lombès[2], Robert P. Martin[1], Nina Entelis[1*], Ivan Tarassov[1*]

[1] Department of Molecular and Cellular Genetics, UMR Génétique Moléculaire, Génomique, Microbiologie (GMGM), CNRS - Université de Strasbourg, Strasbourg, France;

[2] Centre de Recherche de l'Institut du Cerveau et de la Moëlle (CRICM); INSERM UMRS 975, CNRS UMR 7225, UPMC, Paris, France.

[*] corresponding authors : UMR7156 CNRS-Université de Strasbourg, 21 rue René Descartes 67084, Strasbourg, France
Tel. (+33) 3 90 24 14 60
Fax (+33) 3 88 41 70 70
E-mails: i.tarassov@unistra.fr
n.entelis@unistra.fr

[&] these authors contributed equally to this work.
[#] current address: AP/HP Hôpital Ambroise Paré, Boulogne-Billancourt, France
[§] current address: Institut für Molekulare Infektionsbiologie, Josef Schneider-Str. 2 / D1597080 Würzburg, Germany

Content: **Table S1**

Figures S1 - S9

Table S1. Oligonucleotides used in the study.

Name	Sequence, 5'>3'	Purpose
FDpcr	AAGAGCCCTGTAGGG	FD-RNAs detection
T7pr	GGGATCCATAATACGACTCACTATA	T7 promotor
1095 F	TAGCCCTAAACCTCAACAGT	qPCR for 12S rRNA gene quantification
1305B	TGCGCTTACTTTGTAGCCTTCAT	qPCR for 12S rRNA gene quantification
11614F	CATTGCATACTCTTCAATCAGC	qPCR for KSS deletion quantification
11778B	CGACTGTGAGTGCGTT	qPCR for KSS deletion quantification
Control RNA	GAGAACTAAGCACTG	Control RNA detection by Northern hybridization
FD	GAGTCATACGCGCTACCGATTGCGCCAACAAGGC	FD-RNAs detection by Northern hybridization, homology to the D-arm of tRK1
15251-15680F	CTTAAAGCTTCACACGATTCTTTACCTTTC	Cloning of the WT mtDNA fragment 15251-15680, forward
15251-15680R	TCTTTGGAATTCGTTTGGATATATGGAGGATGG	Cloning of the WT mtDNA fragment 15251-15680, reverse
8099-8365/15438-15680F	TACTACAAGCTTACAGATGCAATTCCCGGACG	Cloning of the KSS mtDNA fragment 8099-8365/15438-15680, forward
8099-8365/15438-15680R	TCTTTGGAATTCGTTTGGATATATGGAGGATGG	Cloning of the KSS mtDNA fragment 8099-8365/15438-15680, reverse
5.8S Hm F/T7	TAGATCTAATACGACTCACTATAGACTCTTAGCGGTGG	RT-PCR of 5.8S rRNA
5.8S Hm R	GGCCGCAAGTGCGTTCGAAG	Northern hybridization and RT-PCR of 5.8S rRNA
KSSrtF	CCTGAATACAGTGCTTAC	RT-PCR 5S-KSS-L
KSSrtR	CCTGAAAAGTAAGCACTG	RT-PCR 5S-KSS-H
KSS-F-bio	biotin-TCAGTAGACAGTCCCACCCTC	purification of ssDNA-KSS, forward
WT-F-bio	biotin-ACAGATGCAATTCCCGGACG	purification of ssDNA-WT, reverse
R-bio	biotin-GTTTGGATATATGGAGGATGG	purification of ssDNA-KSS, reverse
HmLmit	GAACCTCTGACTGTAAAG	mt-tRNA-Leu detection by Northern hybridization
Actin-F	TCACCCACACTGTGCCCATCTACGA	qPCR quantification of nuclear DNA
Actin-R	CAGCGGAACCGCTCATTGCCAATGG	qPCR quantification of nuclear DNA

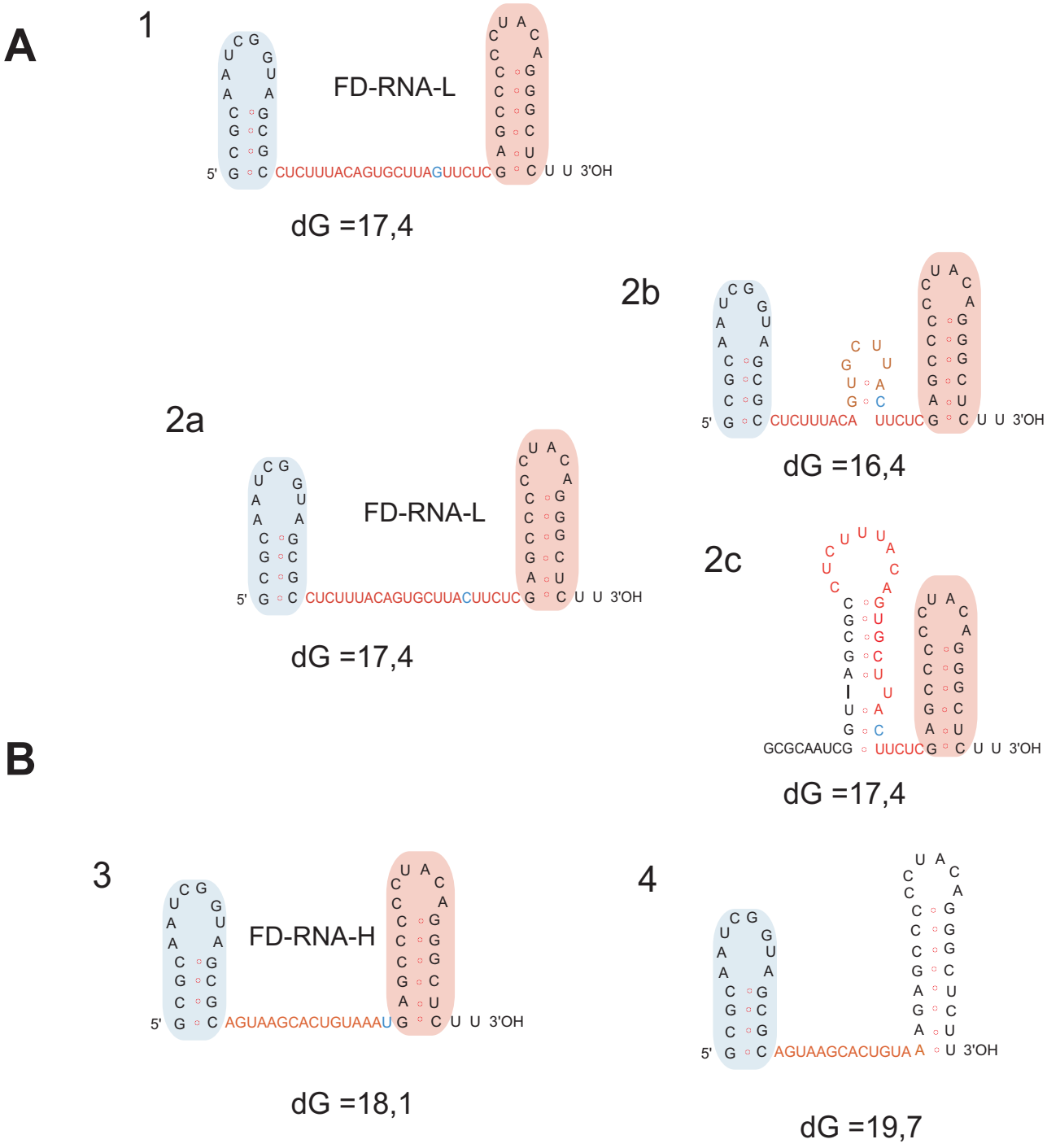

Figure S1. Design of FD RNA-based mitochondrial vectors. The free energy (dG) of each RNA is indicated below in kcal/mol. (**A**) Secondary structure of FD-RNA-L predicted by Mfold. The structure n˚1 corresponds to the FD RNA L in which the 17th C of insertion is replaced by G (in blue), leading to only one structure. The predicted alternative structures 2a,b,c correspond to the FD RNA L without this mismatch. (**B**) Secondary structure of FD-RNA-H predicted by Mfold. The structure n˚3 corresponds to the molecule in which an U has been introduced between the 3' part of the insert and the F helix (shown in blue). n˚4 corresponds to the secondary structure of FD RNA H without additional U.

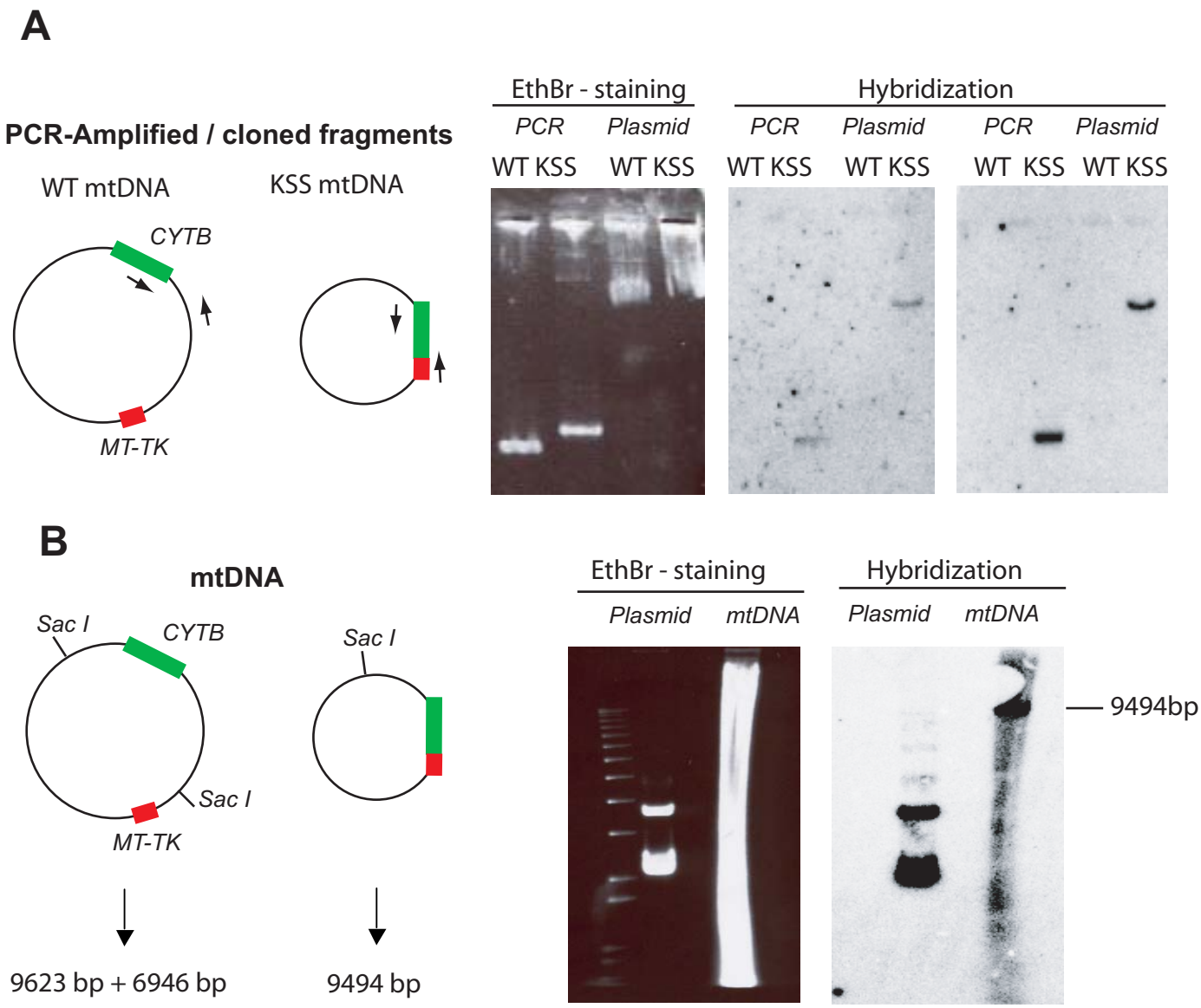

Figure S2. Analysis of the specificity of FD-L and FD-H RNAs interaction with mutant mtDNA by Southern hybridisation. (**A**) Hybridization of 32P-labeled RNAs with PCR-ampified fragment containing either the KSS deletion boarders or a nearby localized WT mtDNA sequence (localization of the primers is indicated by the arrows in the left picture). (**B**) Hybridisation of labeled FD-L RNA with *Sac*I-cleaved mtDNA and (as control) with the plasmid containing KSS deletion boundary region. At the left, restriction maps of WT and KSS mtDNA. MT-TK, the tRNA(Lys) gene.

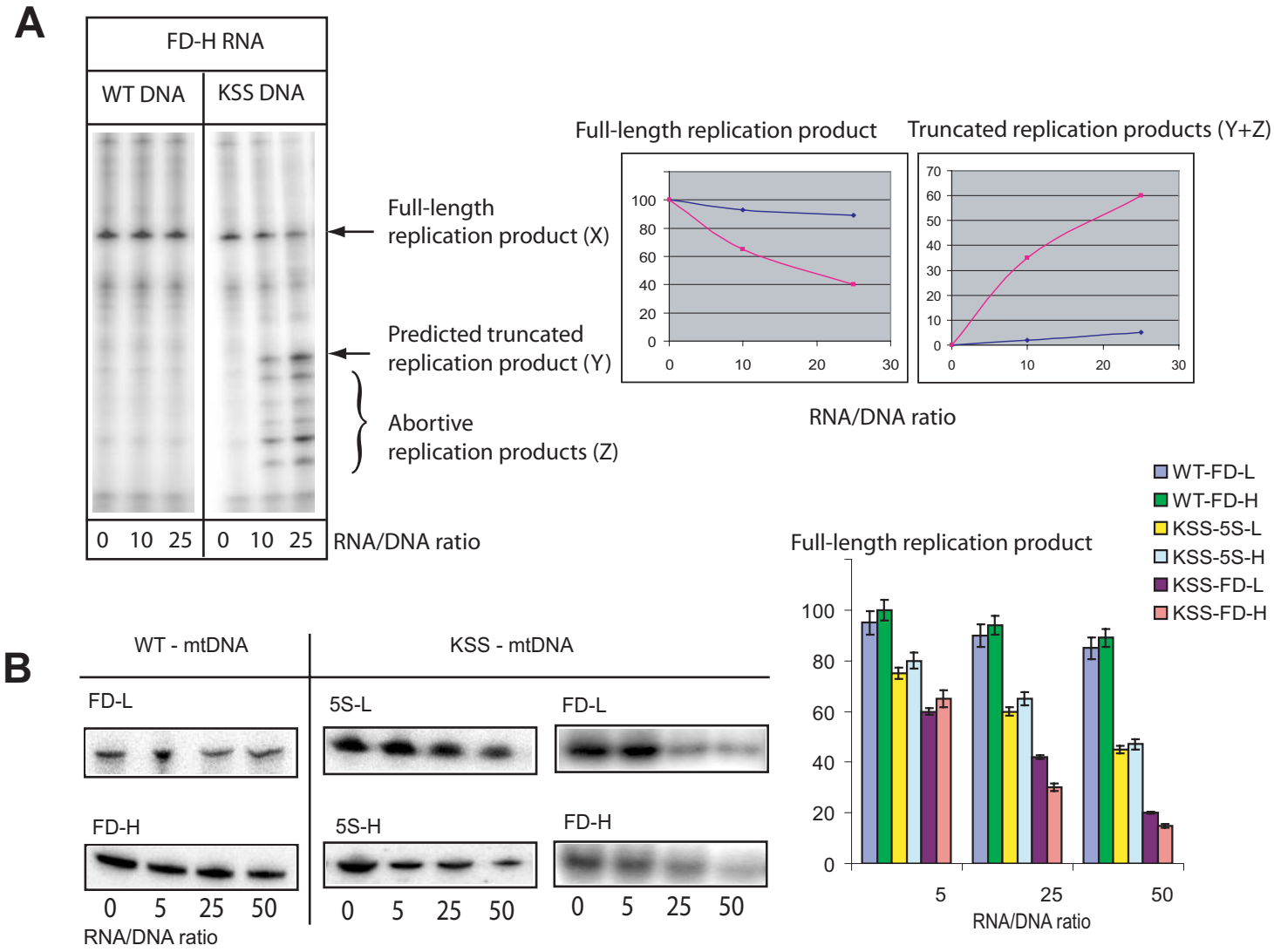

Figure S3. The effect of recombinant RNA on mtDNA replication in vitro. Replication run-off assay comprised PCR-amplified mtDNA fragments containing wild-type mtDNA or KSS-mtDNA sequences, [32P]-5'-labeled specific primers and a mitochondrial protein fraction containing replication enzymes obtained from beef liver mitochondria. (A) Autoradiography of denaturing PAGE demonstrating in vitro replication of KSS or wild type mtDNA fragments in the presence of increasing amounts of FD-H recombinant RNA. RNA/DNA molar ratio is shown below the panel. Several bands of intermediate abortive replicaton products (Z) can appear due to degradation of the main truncated product of predicted size (Y). The graphs at the right represent the relative amounts of mtDNA replication products upon increasing amounts of FD-H RNA, 100%, replication in absence of RNA. (B) The anti-replication effect of various recombinant RNAs. Only the full-size replication product is shown and quantified here. The autoradiograph represent one of the experiments, the diagrams at the right result from 4 independent experiments.

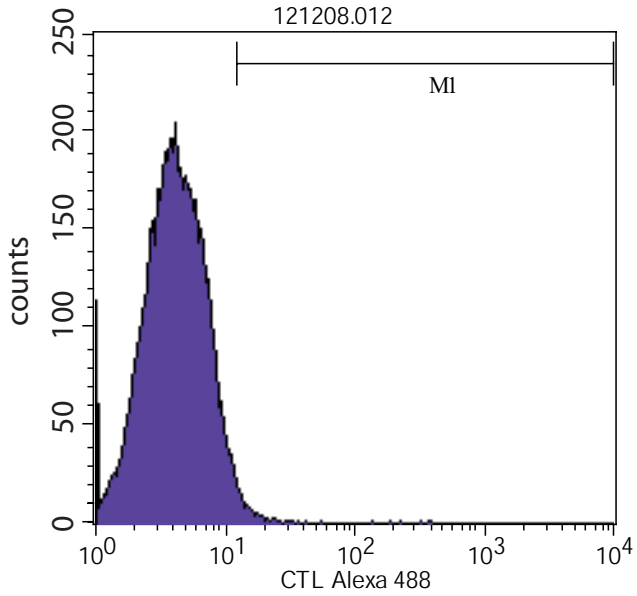

Sample ID: TSFR CTL Gate: G1
Gated Events: 25727

Marker	Events	% Gated	% Total	Mean	Geo Mean
All	25727	100.00	86.49	4.67	4.06
M1	278	1.08	0.93	20.90	16.08

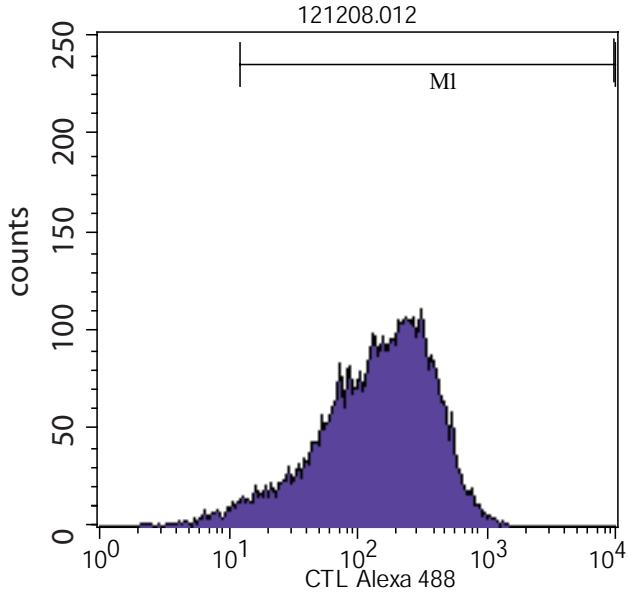

Sample ID: TSFR Optimem Fluo Gate: G1
Gated Events: 22539

Marker	Events	% Gated	% Total	Mean	Geo Mean
All	22539	100.00	83.06	196.43	136.17
M1	22135	**98.21**	81.57	199.85	143.26

Figure S4. Verification of the efficiency of cybrid cells transient transfection with FD-L RNA by FACS. X-axis indicates the number of collected cells, Y-axis - the intensity of fluorescence. The upper pannel corresponds to cells transfected with non-fluorescent RNA, while the bottom one - to cells transfected with FD-L RNA labeled by Alexa 488. The percentage of fluorescent cells present in the selected window M1 is outlined by a red square.

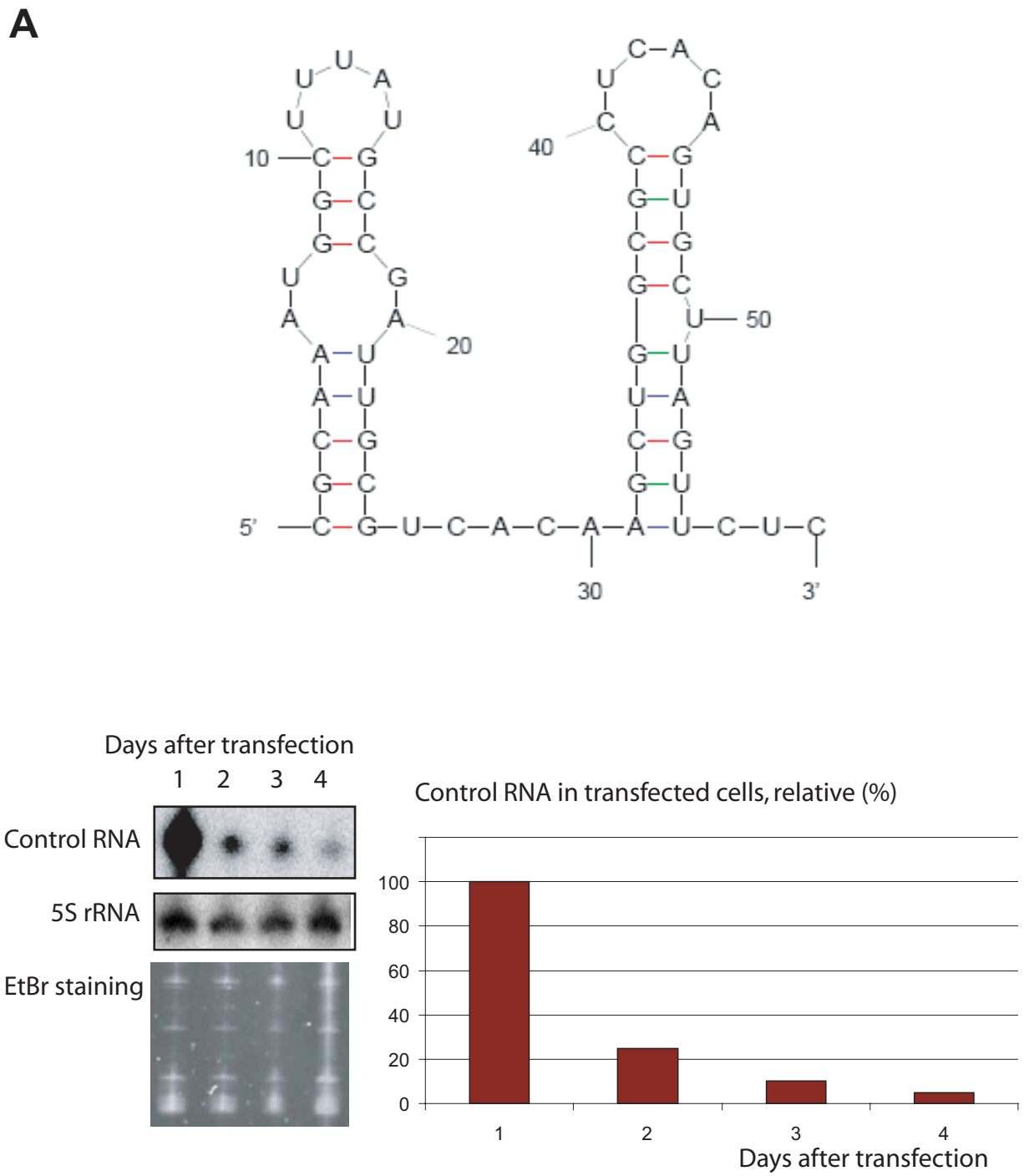

Figure S5A. Analysis of the stability of the control non-imported RNA in transfected KSS cybrid cells. Upper pannel : predicted secondary structure of the control RNA. Bottom pannel: Northern hybridisation of total RNA extracted from transiently transfected cells with ^{32}P-labeled RNA-specific probe (Control RNA) and 5S rRNA probe (as a quantitative control). At the lower panel, Ethidium Bromide staining of the same gel is shown. The graph at the right represents the time-dependence of RNA decay (as in Fig. 3A, see Methods for details). Detected amount of RNA at day 1 compared to day 2 after transfection is very important, probably due to attachment of RNA-containing Lipofectamin granules on the cell surface, thus, this value can be over-estimated. The rate of Control RNA degradation in cybrid cells in 2, 3 and 4 days after transfection is comparable to those of imported FD-RNAs (Fig. 3A), so the absence of Control RNA in the mitochondria in 2 days after transfection (Fig. 3B) proves the selectivity of RNA import process.

B

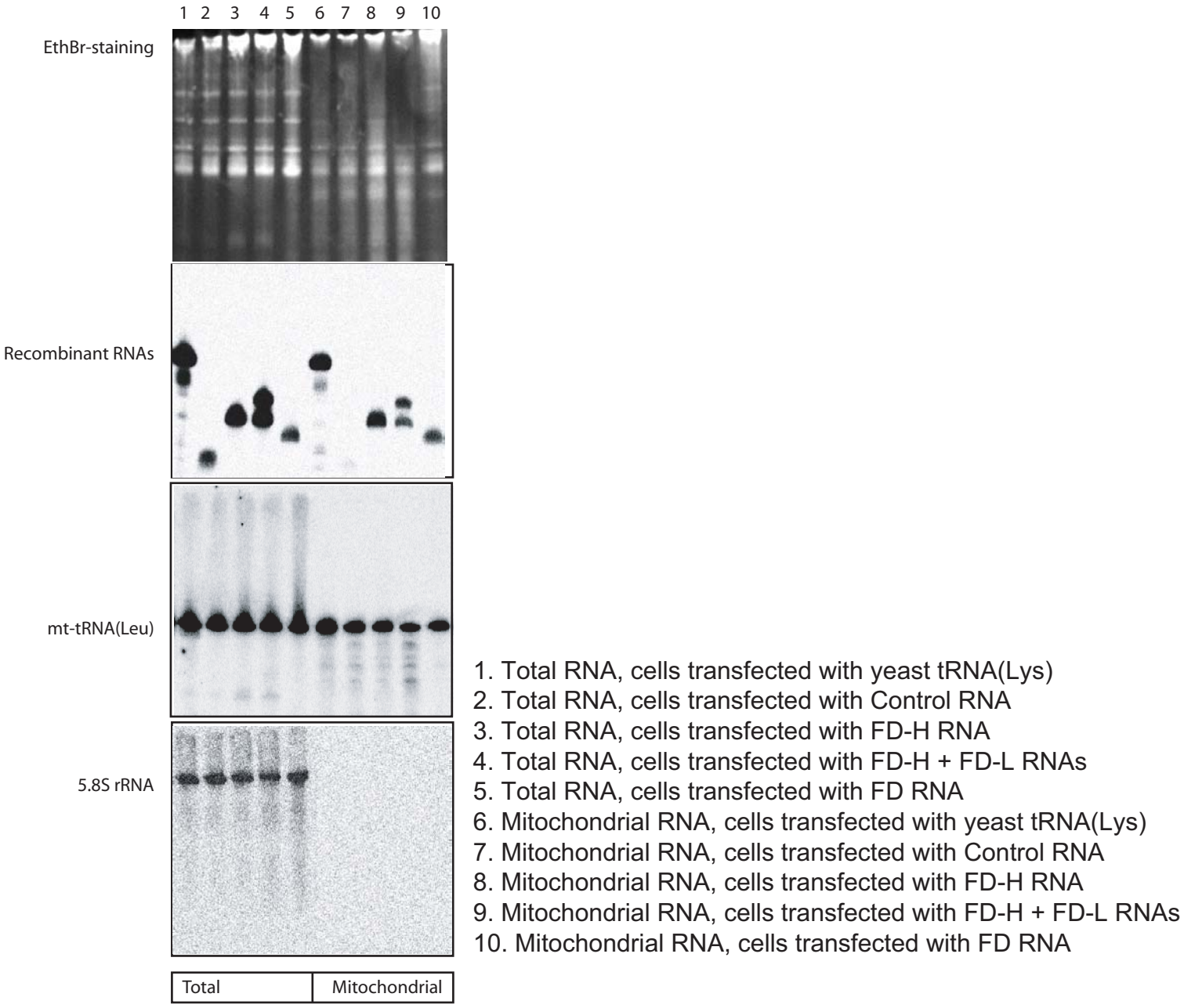

Figure S5B. Mitochondrial import of recombinant FD-RNAs in transiently transfected cybrid cells. An example of urea-PAGE separation (upper panel) and hybridisation analysis of RNA isolated from cells (lanes 1-5) and purified mitochondria (lanes 6-10), as indicated below, 2 days after transfection with RNA indicated at the right. Hybridisation probes are indicated at the left. The signals in the mitochondrial fraction are weaker with the probe to mt-tRNA as compared to the total sample, indicating on the partial loss of mtRNA during the mitochondria isolation and purification.Total RNA samples were isolated from the twice less amount of cultured human cells comparing to starting material for mitochondria purification (25 cm2 of cells).

A

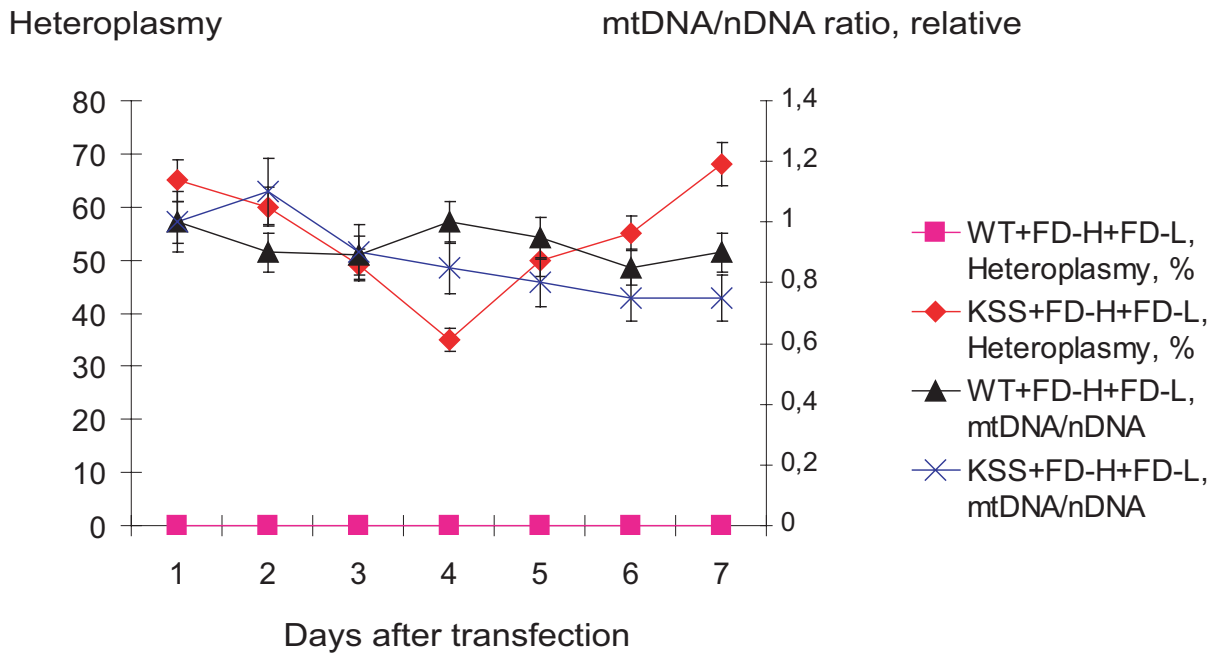

B

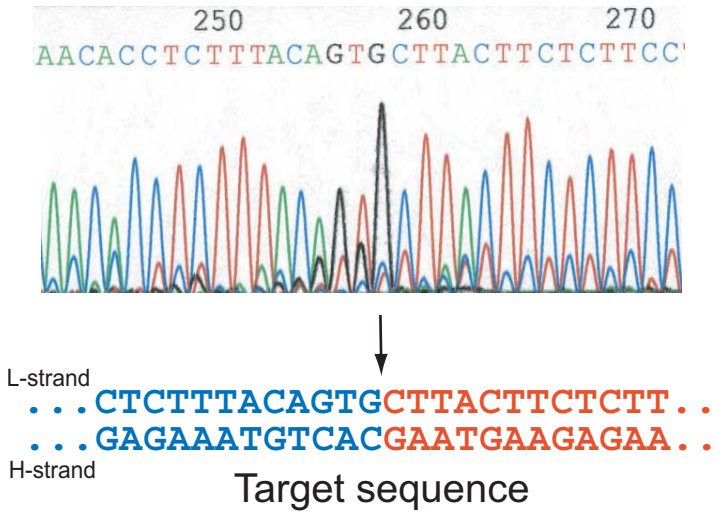

Figure S6 A. Results of real-type qPCR analysis of heteroplasmy levels (at the left) and of the ratio between mitochondrial and nuclear DNA (at the right) in wild type (WT) and KSS cybrid cells (KSS) transfected with two recombinant anti-replicative RNAs, FD-H and FD-L. **B**. Analysis of the stability of the KSS deletion joint point in transfected cybrid cells. An example of the PCR-amplified mtDNA sequence is presented, which demonstrate the absence of heterogeneity of the inititial deletion boundaries. Such verifications were systematically performed at different time points after transient transfection, as well as in stably transfected clones.

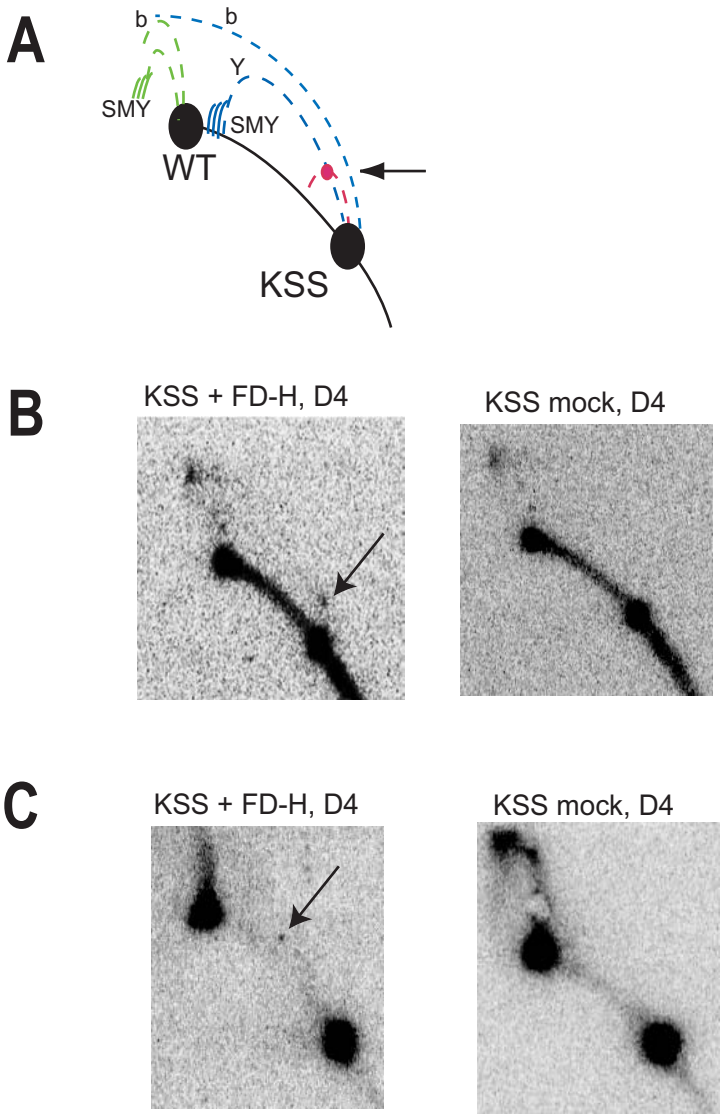

Figure S7. Recombinant RNA affects mutant mtDNA replication in vivo. (A) Schematic representation of replication intermediates (RI): in green, RI corresponding to wild type mtDNA; in blue, corresponding to mutant mtDNA. b, bubble arcs; Y, y arc; SMY, slow migrating y arcs. (B,C) Native 2D agarose gel electrophoretic analysis of mtDNA isolated from KSS cybrid cells. MtDNA was digested with BlpI, blotted and hybridised with P32 labelled fragment of the Cyt b gene (as in Fig.4). Results of two undependent experiments are presented, left panels - mtDNA isolated from cells in 4 days after transfection with anti-replicative RNA FD-H; right panels - mtDNA from mock-transfected cells (treated with Lipofectamin but without any RNA), isolated and separated in the same conditions as one presented at the left. The site of replication pausing, visible only in cells transfected with FD-H RNA, is shown by arrow.

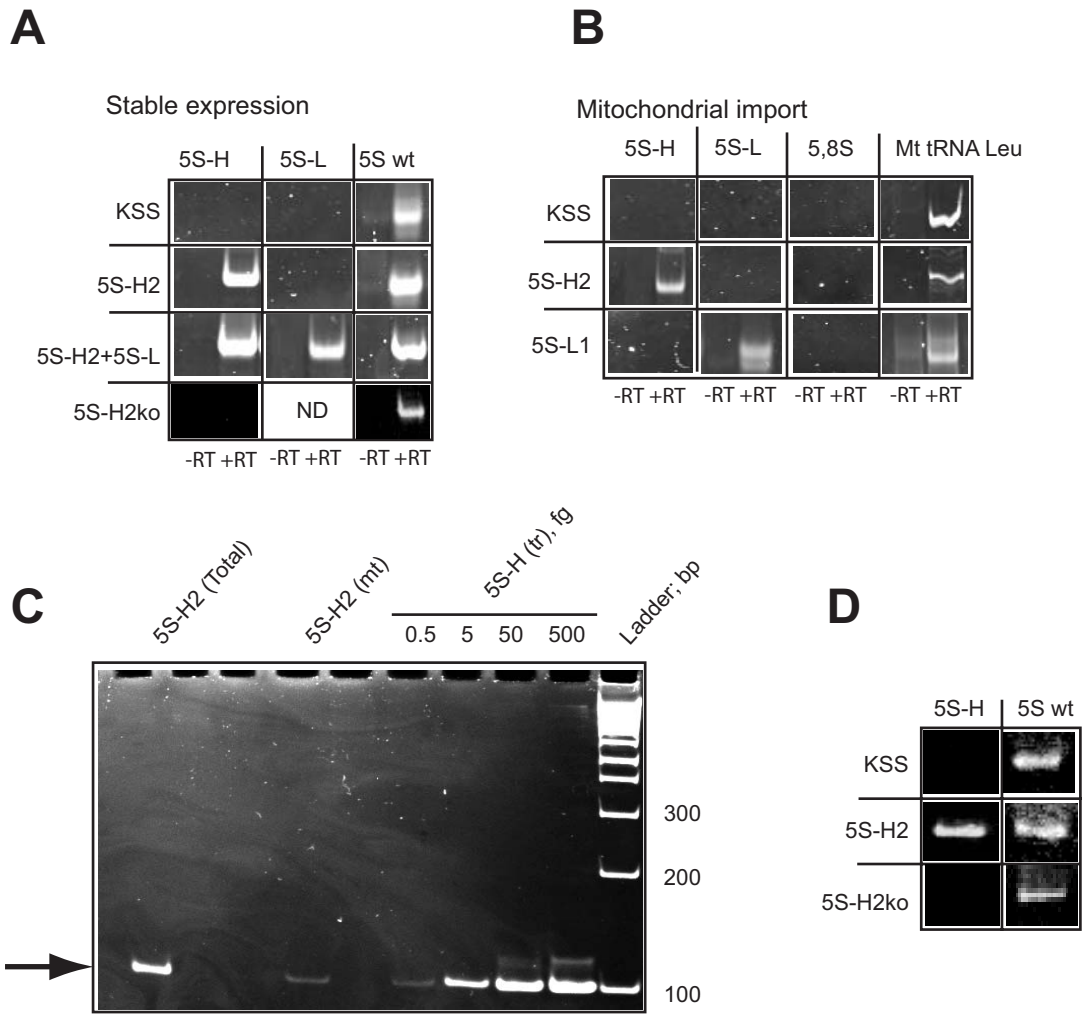

Figure S8. Expression and import of recombinant RNAs in stable clones. (A) RT-PCR analysis of expression of 5S-H or both recombinant 5S RNAs in stable cell lines. (B) Mitochondrial import of recombinant 5S rRNAs detected by RT-PCR. Amplified RNAs are indicated above the panel, cell lines are shown at the left: KSS, mock-transfected cells; 5S-H2, clone expressing 5S-H RNA; 5S-L1, clone expressing 5S-L RNA; 5S-H2ko, subclone of 5S-H2 which has lost 5S-H RNA expression. -RT, control without reverse transcriptase. ND, non-determined. (C) Semi-quantitative RT-PCR of 5S-H in the stable clone 5S-H2. RNA samples coresponding to known amount of cells (Total) or mitochondria (mt) were analysed, in parallel with fixed amounts of the corresponding T7-transcript. Full-size PCR product is indicated by the arrow. (D) PCR analyses of the presence of the transgene in the 5S-H2ko cell line.

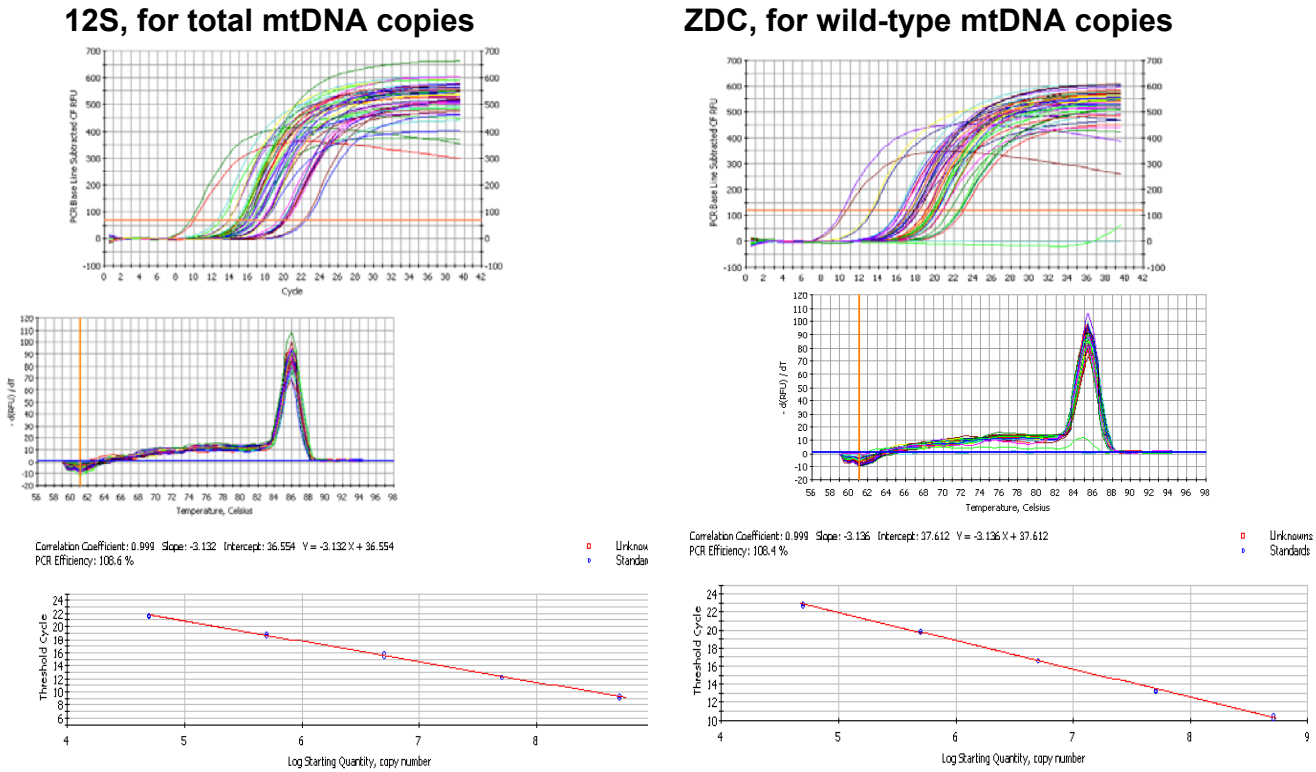

Identifier	SQ Mean	SQ Std. Dev.	Ct Mean	Ct Std. Dev.	SQ zdc/12s	correction	**KSS deletion**
	12S for total mtDNA						
WT	1,32E+07	1,24E+06	15,02	1,36E-01	5,67E-01	1,00E+00	**0%**
Mt	2,52E+06	9,96E+04	17,39	5,67E-02	2,05E-01	3,61E-01	**64%**
clone 5S-H5	5,88E+06	5,50E+05	16,18	1,37E-01	2,96E-01	5,22E-01	**48%**
clone 5S-H8	1,23E+07	1,14E+06	15,12	1,34E-01	3,14E-01	5,54E-01	**45%**
clone 5S-H7	9,44E+06	4,87E+05	15,5	7,40E-02	3,26E-01	5,76E-01	**42%**
clone 5S-H2	1,82E+07	2,29E+06	14,56	1,82E-01	3,76E-01	6,64E-01	**34%**
	ZDC for wt mtDNA						
WT	7,49E+06	3,58E+05	15,25	6,89E-02			
Mt	5,16E+05	5,05E+04	19,15	1,43E-01			
clone 5S-H5	1,74E+06	1,07E+05	17,37	8,85E-02			
clone 5S-H8	3,86E+06	2,04E+05	16,21	7,71E-02			
clone 5S-H7	3,08E+06	3,03E+04	16,54	1,43E-02			
clone 5S-H2	6,85E+06	4,10E+05	15,38	8,57E-02			

Figure S9. An example of the real-time qPCR experiment. 12S and ZDC, two pairs of primers, amplifying the 210 bp fragment of 12S rRNA gene region as a value showing all mtDNA molecules, and the 164 bp fragment of the deleted region (ZDC for Common Deletion Zone) as a value showing only wild type mtDNA molecules. On the middle panels, the melting curves following 40 cycles of amplification are presented. Lowed panels represent the standard calibration curves, obtained with 5 serial dilutions of linearized plasmid DNA (10^4-10^7 copies per sample). The same DNA was used to set up standard curve reactions in every plate in the study. Below the panels, experimental data and heteroplasmy calculation for DNA isolated from clones expressed 5S-H RNA. WT and Mt, DNA isolated from wild-type and cybrid KSS cells. Ct, Threshold cycle; SQ, Starting Quantity. Mean values and standard deviations (Std. Dev.) were estimated from analysis of each sample in triplicate.